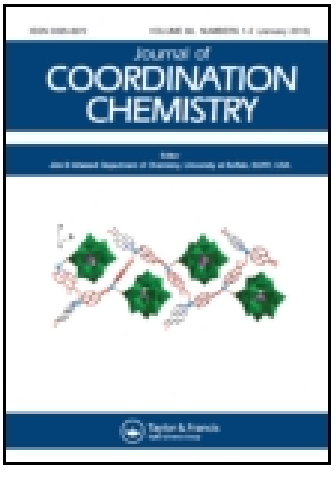

Journal of Coordination Chemistry
Publication details, including instructions for authors and subscription information:
http://www.tandfonline.com/loi/gcoo20

Homochiral imidazole-based dicarboxylate metal complexes with $SrSi_2$ topology: synthesis, crystal structures, and properties

Li Sun[a], Jiang-Feng Song[a], Rui-Sha Zhou[a], Jia Zhang[a], Lu Wang[a], Kun-Li Cui[a] & Xiao-Yu Xu[b]

[a] Department of Chemistry, North University of China, Taiyuan, PR China

[b] Department of Public Security of Jilin Province, Changchun, PR China

Accepted author version posted online: 10 Mar 2014.Published online: 04 Apr 2014.

To cite this article: Li Sun, Jiang-Feng Song, Rui-Sha Zhou, Jia Zhang, Lu Wang, Kun-Li Cui & Xiao-Yu Xu (2014) Homochiral imidazole-based dicarboxylate metal complexes with $SrSi_2$ topology: synthesis, crystal structures, and properties, Journal of Coordination Chemistry, 67:5, 822-836, DOI: 10.1080/00958972.2014.902448

To link to this article: http://dx.doi.org/10.1080/00958972.2014.902448

Journal of Coordination Chemistry, 2014
Vol. 67, No. 5, 822–836, http://dx.doi.org/10.1080/00958972.2014.902448

Homochiral imidazole-based dicarboxylate metal complexes with $SrSi_2$ topology: synthesis, crystal structures, and properties

LI SUN†, JIANG-FENG SONG*†, RUI-SHA ZHOU†, JIA ZHANG†, LU WANG†, KUN-LI CUI† and XIAO-YU XU‡

†Department of Chemistry, North University of China, Taiyuan, PR China
‡Department of Public Security of Jilin Province, Changchun, PR China

(*Received 13 January 2013; accepted 4 January 2014*)

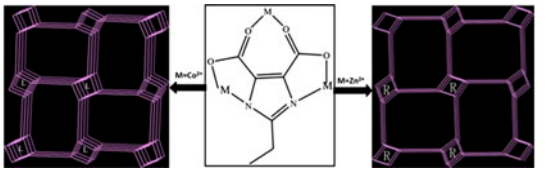

Two novel homochiral frameworks with $SrSi_2$ topology, $\{Co_3(EIDC)_2(H_2O)_5\}_n$ (**1**) and $\{Zn_3(EIDC)_2(H_2O)_4\}_n$ (**2**) (H_3EIDC = 2-ethyl-1H-imidazole-4,5-dicarboxylic acid), have been synthesized from totally achiral starting precursors via spontaneous resolution. The homochiral natures of **1** and **2** were further confirmed by circular dichroism spectra.

Two new complexes with homochiral frameworks, $\{Co_3(EIDC)_2(H_2O)_5\}_n$ (**1**) and $\{Zn_3(EIDC)_2(H_2O)_4\}_n$ (**2**) (H_3EIDC = 2-ethyl-1H-imidazole-4,5-dicarboxylic acid), have been synthesized from achiral starting precursors via spontaneous resolution and fully characterized by elemental analyses, IR, circular dichroism, photoluminescence (PL) spectroscopy, single-crystal X-ray diffraction, and thermogravimetric analysis. X-ray diffraction data revealed that **1** and **2** have $SrSi_2$ topologies and that both are homochiral metal–organic frameworks. Compound **1** is constructed by left-handed chiral chains; however, right-handed chains constitute the homochiral framework of **2**. Variable temperature magnetic susceptibility measurements of **1** indicate strong antiferromagnetic interactions between the magnetic Co centers. Compound **2** exhibited weak blue PL in the solid state at room temperature.

Keywords: Homochirality; Coordination polymer; Crystal structure; Fluorescence; Magnetic property

1. Introduction

Coordination polymers (CPs) have attracted attention due to their intriguing structures and potential applications in storage, separation, catalysis, and biomedical and sensor materials

*Corresponding author. Email: jfsong0129@nuc.edu.cn

[1–13]. Selection of organic linkers has the most important impact on the building of CPs. Recently, 4,5-imidazole dicarboxylate (H_3IDC) and its analogs, such as 2-methyl-1H-imidazole-4,5-dicarboxylic acid, 2-ethyl-1H-imidazole-4,5-dicarboxylic acid (H_3EIDC), and 2-propyl-1H-imidazole-4,5-dicarboxylic acid, have drawn attention in preparation of intriguing CPs [14–45]. These linkers are good multidentate N- or O-donors with various coordination modes and act as H-bond acceptors and donors to assemble various supramolecular structures. They can also be partly or fully deprotonated depending on the pH, providing various acid–base type coordination modes. The two nitrogens in the imidazole ring can gear the coordination orientation, consistent with Si–O–Si bond angles in zeolites or M–IM–M bond angle in zeolitic imidazolate frameworks [46, 47].

By the analysis of CPs constructed by H_3IDC or its analogs [14–45], we found that many CPs based on chiral chains were reported [17, 40–45]; however, most of them contain both left-handed and right-handed helical chains, resulting in the formation of achiral frameworks. To the best of our knowledge, the only reported homochiral frameworks based on H_3IDC or its analogs are $\{K[Cd(EIDC)]\}_n$ and $Co_3(tmidc)_2(H_2O)_4]\cdot(H_2O)_4$ (H_3tmidc = 2-((1H-1,2,4-triazol-1-yl)methyl)-1H-imidazole-4,5-dicarboxylic acid) [17, 40]. These two CPs are synthesized by spontaneous resolution, which is an effective approach to synthesize homochiral CPs from achiral reaction precursors [48, 49]. As part of our ongoing efforts in the design and synthesis of crystalline materials based on analogs of H_3IDC [33], here we report the synthesis, crystal structures, and properties of two homochiral CPs, $\{Co_3(EIDC)_2(H_2O)_5\}_n$ (**1**) and $\{Zn_3(EIDC)_2(H_2O)_4\}_n$ (**2**), which are obtained from totally achiral starting precursors via spontaneous resolution. Compounds **1** and **2** are 3-D 3-connected nets with $SrSi_2$ topology. Interestingly, **1** is constructed by left-handed chains and a 3-D metal–water network further stabilizes the homochiral framework; however, right-handed chains constitute the homochiral framework of **2**, which is stabilized by 1-D metal–water chains.

2. Experimental setup

2.1. *Materials and methods*

All chemicals and solvents were of reagent grade, purchased and used without purification except H_3EIDC, which was prepared according to a literature procedure [50]. C, H, and N elemental analyses were performed on a Perkin-Elmer 240C elemental analyzer. IR spectra were measured on a Perkin-Elmer Spectrum One FT-IR spectrometer using KBr pellets. Powder X-ray diffraction (PXRD) patterns of the samples were recorded on a RIGAKU-DMAX2500 X-ray diffractometer with Cu Kα radiation. Circular dichroism (CD) spectra of solid samples were recorded between 190 and 600 nm at room temperature with a J-715 spectrometer as KBr pellets. Thermogravimetric analyses (TGA) were performed on a Perkin-Elmer TGA-7000 thermogravimetric analyzer under flowing air at a temperature ramp rate of 10 °C min^{-1}. Photoluminescence (PL) excitation and emission spectra were recorded at room temperature with a Jobin Yvon Fluoro Max-4 spectrophotometer equipped with a 150 W xenon lamp as the excitation source. Variable temperature magnetic susceptibility measurements were carried out using a MPMS XL-7 SQUID magnetometer (Quantum Design) at 1.0 kOe from 2 to 300 K. SEM–EDS microanalysis was carried out with a JSM-7500F scanning electron microscope equipped with EDS microanalysis system.

2.2. *Synthesis of 1 and 2*

2.2.1. Synthesis of 1. A solution of H_3EIDC (18.5 mg, 0.1 mM) in 4 mL water containing $NH_2NH_2{\cdot}H_2O$ (50 µL, 50 wt%) was mixed with a solution of $Co(NO_3)_2{\cdot}6H_2O$ in 2 mL water (0.10 M L^{-1}) at room temperature in a 15 mL beaker. A solution of 3,6-di-4-pyridyl-1,2,4,5-tetrazine (DPT, 11.8 mg, 0.05 mM) in 2 mL methanol was added to the reaction mixture. Then, CH_3COOH was added until the pH was 6. The resulting mixture was transferred to, and sealed in, a 25 mL Teflon-lined stainless steel reactor and heated at 170 °C for 72 h. Upon cooling to room temperature, a clear pink solution, red crystals, and a lightweight black precipitate (about 2 mg) were obtained. The crystals were isolated by filtration and washed with water and ethanol. Yield: 65% (based on H_3EIDC). Elem. Anal. Calcd $C_{14}H_{20}Co_3N_4O_{13}$ (629.13): C, 26.70; H, 2.22; N, 8.90. Found: C, 26.62; H, 2.29; N, 8.79. IR data (KBr, cm^{-1}): (w = weak, m = medium, s = strong). 3254(s), 2974(w), 1564(s), 1449(s), 1367(s), 1263(m), 1128(s), 1056(w), 879(w), 796(m), 744(w).

In a control experiment, the same procedure was followed except that DPT was not added. Upon cooling to room temperature, a pink precipitate and a small amount of red crystals consistent with **1** (yield: 5.6%, based on H_3EIDC) were obtained.

2.2.2. Synthesis of 2. The procedure was the same as that for **1** except that $Co(NO_3)_2{\cdot}6H_2O$ was replaced by $ZnCl_2$. Upon cooling to room temperature, a clear yellow solution and colorless crystals were obtained. The crystals were filtered and washed with water and ethanol. Yield: 52% (based on H_3EIDC). Elem. Anal. Calcd $C_{14}H_{18}Zn_3N_4O_{12}$ (630.43): C, 26.65; H, 2.86; N, 8.88. Found: C, 26.69; H, 2.95; N, 8.79. IR data (KBr, cm^{-1}): (w = weak, m = medium, s = strong). 3389(s), 2974(w), 1574(s), 1449(s), 1264(m), 1056(w), 879(w), 796(m), 744(w).

In a control experiment, the same procedure was followed except that DPT was not added. Upon cooling to room temperature, only a yellow precipitate was obtained.

2.3. *Crystal structure determination*

The crystal structures were determined by single-crystal X-ray diffraction. Reflection data were collected on a Bruker SMART CCD area-detector diffractometer (Mo-Kα radiation, graphite monochromator) at room temperature with ω-scan mode. Empirical adsorption corrections were applied to all data using SADABS. The structure was solved by direct methods and refined by full-matrix least squares on F^2 using SHELXTL 97 software [51]. Non-hydrogen atoms were refined anisotropically. All C-bound hydrogens were refined using a riding model. Hydrogens of water (O1w, O2w, and O3w for **1**; O3w for **2**) were located in a difference Fourier map and their positions were refined under the application of an O−H bond-length restraint of 0.85 Å; however, hydrogens for O1w, O2w, and O4w in **2** were not located. All calculations were carried out using SHELXTL 97 [51] and PLATON [52]. The crystallographic data and pertinent refinement parameters are given in table 1 and selected bond distances and angles in table 2. The geometric parameters of the hydrogen bonds in **1** and **2** are listed in table S1 (see online supplemental material at http://dx.doi.org/10.1080/00958972.2014.902448).

Table 1. Crystal data and structure refinement for **1** and **2**.

Complex	**1**	**2**
Empirical formula	$C_{14}H_{20}Co_3N_4O_{13}$	$C_{14}H_{18}N_4O_{12}Zn_3$
Formula weight	629.13	630.43
Crystal system	Tetragonal	Orthorhombic
Space group	$P4_32_12$	$P2_12_12_1$
a, Å	9.9837 (14)	9.7488 (19)
b, Å	9.9837 (14)	10.196 (2)
c, Å	21.870 (4)	22.182 (4)
α, °	90	90
β, °	90	90
γ, °	90	90
Volume (Å^3)	2179.9(6)	2204.7(8)
Z	4	4
ρ_{Calcd}/g cm^{-3}	1.917	1.899
Absorption coeff./mm^{-1}	2.331	3.306
θ Range (°)	3.03 27.43	3.03−27.48
Reflections collected	21,148	20,730
Unique reflections (R_{int})	2490 (0.0515)	4939 (0.0801)
Goodness-of-fit on F^2	1.253	1.038
R indexes [$I > 2\sigma(I)$][a]	$R_1 = 0.0576$, $wR_2 = 0.1216$	$R_1 = 0.0618$, $wR_2 = 0.1532$
R (all data)[a]	$R_1 = 0.0592$, $wR_2 = 0.1222$	$R_1 = 0.0750$, $wR_2 = 0.1636$
Flack parameters	0.04(4)	0.05(3)

[a]$R_1 = \Sigma||F_o| - |F_c||/\Sigma|F_o|$; $wR_2 = [\Sigma w(F_o^2 - F_c^2)_2/\Sigma w(F_o^2)^2]^{1/2}$.

3. Results and discussion

3.1. *Synthesis*

CPs **1** and **2** with homochiral frameworks were prepared through reactions of H_3EIDC, DPT, and Co or Zn under solvothermal conditions. A small amount of a black precipitate and **1** in high yield were obtained. The morphology and composition of the black precipitate were determined by SEM and EDX, respectively. As shown in figure S1, the EDX plot from the black precipitate revealed C, O, N, and Co signals of 38.45, 38.06, 14.59, and 8.90 wt%, respectively. In the control experiment without DPT, a small amount of red crystals was obtained and no black precipitate was found. The PXRD pattern (figure S2) of the red crystals is consistent with that for **1**, suggesting that **1** was obtained in the control experiment. It may be concluded that DPT has an important influence on the yield and crystal growth for **1** and **2;** however, the explicit effect of both the hydrazine and DPT in these syntheses is unknown.

3.2. *Crystal structure*

3.2.1. Crystal structure of 1. X-ray crystallographic data revealed that **1** has a 3-D homochiral framework and crystallized in the chiral space group $P4_32_12$. The asymmetric unit of **1** contains 1.5 Co^{2+} cations, a μ_3-$EIDC^{3-}$, and 2.5 coordinated waters. Co2 is located on a twofold axis, so the corresponding occupancy is 0.5. As shown in figure 1(a), Co1 shows a disordered octahedral coordination geometry where the equatorial plane is occupied by one carboxylate (O1) and one N (N1a, symmetry code: a, $0.5 + y$, $1.5 - x$, $0.25 + z$) from two symmetrically equivalent $EIDC^{3-}$ anions, together with two coordinated waters (O1w and O2w). The axial groups are carboxylate O3a and O4 from two symmetrically equivalent

Table 2. Bond lengths (Å) and angles (°) for **1** and **2**.

1			
Co(1)–O(4)	2.004 (5)	O(3)#1–Co(1)–O(2W)	95.2 (2)
Co(1)–O(3)#1	2.073 (4)	N(1)#1–Co(1)–O(2W)	87.2 (2)
Co(1)–N(1)#1	2.088 (6)	O(1)–Co(1)–O(2W)	179.1 (2)
Co(1)–O(1)	2.103 (5)	O(4)–Co(1)–O(1W)	87.8 (2)
Co(1)–O(2W)	2.127 (6)	O(3)#1–Co(1)–O(1W)	85.48 (19)
Co(1)–O(1W)	2.142 (5)	N(1)#1–Co(1)–O(1W)	162.7 (2)
Co(2)–O(3)	1.984 (7)	O(1)–Co(1)–O(1W)	93.5 (2)
Co(2)–N(2)	2.002 (6)	O(2W)–Co(1)–O(1W)	86.8 (2)
Co(2)–O(2)	2.148 (5)	O(3W)–Co(2)–N(2)	121.25 (18)
O(4)–Co(1)–O(3)#1	172.2 (3)	N(2)#2–Co(2)–N(2)	117.5 (4)
O(4)–Co(1)–N(1)#1	108.3 (3)	O(3W)–Co(2)–O(2)#2	88.84 (14)
O(3)#1–Co(1)–N(1)#1	78.9 (2)	N(2)–Co(2)–O(2)#2	101.6 (2)
O(4)–Co(1)–O(1)	92.5 (2)	O(3W)–Co(2)–O(2)	88.84 (14)
O(3)#1–Co(1)–O(1)	84.02 (19)	N(2)–Co(2)–O(2)	79.6 (2)
N(1)#1–Co(1)–O(1)	92.3 (2)	O(2)#2–Co(2)–O(2)	177.7 (3)
O(4)–Co(1)–O(2W)	88.3 (2)		
2			
N(1)–Zn(2)	2.016 (7)	O(1)–Zn(1)–O(5)	172.1 (3)
N(2)–Zn(3)	2.022 (7)	N(3)–Zn(1)–O(5)	79.1 (2)
N(3)–Zn(1)	2.050 (6)	O(4)–Zn(1)–O(5)	84.2 (2)
N(4)–Zn(3)#1	2.023 (7)	O(4W)–Zn(1)–O(5)	85.7 (2)
O(1)–Zn(1)	2.021 (5)	O(3W)–Zn(1)–O(5)	95.9 (3)
O(2)–Zn(2)	2.187 (6)	O(7)#3–Zn(2)–O(2W)	123.3 (3)
O(3)–Zn(3)	2.149 (6)	O(7)#3–Zn(2)–N(1)	108.8 (3)
O(4)–Zn(1)	2.093 (6)	O(2W)–Zn(2)–N(1)	123.3 (3)
O(5)–Zn(1)	2.170 (5)	O(7)#3–Zn(2)–O(6)#3	96.2 (2)
O(6)–Zn(2)#2	2.020 (5)	O(2W)–Zn(2)–O(6)#3	88.1 (3)
O(7)–Zn(2)#2	1.971 (6)	N(1)–Zn(2)–O(6)#3	108.3 (3)
O(8)–Zn(3)#1	2.124 (6)	O(7)#3–Zn(2)–O(2)	83.0 (2)
O(1W)–Zn(3)	1.985 (6)	O(2W)–Zn(2)–O(2)	85.4 (2)
O(2W)–Zn(2)	1.981 (6)	N(1)–Zn(2)–O(2)	79.7 (2)
O(3W)–Zn(1)	2.131 (7)	O(6)#3–Zn(2)–O(2)	171.6 (3)
O(4W)–Zn(1)	2.127 (6)	O(1W)–Zn(3)–N(2)	116.6 (3)
O(1)–Zn(1)–N(3)	107.5 (3)	O(1W)–Zn(3)–N(4)#4	128.0 (3)
O(1)–Zn(1)–O(4)	91.0 (2)	N(2)–Zn(3)–N(4)#4	115.4 (3)
N(3)–Zn(1)–O(4)	93.4 (3)	O(1W)–Zn(3)–O(8)#4	87.1 (3)
O(1)–Zn(1)–O(4W)	88.0 (3)	N(2)–Zn(3)–O(8)#4	104.9 (3)
N(3)–Zn(1)–O(4W)	164.3 (2)	N(4)#4–Zn(3)–O(8)#4	80.5 (2)
O(4)–Zn(1)–O(4W)	88.5 (3)	O(1W)–Zn(3)–O(3)	86.5 (3)
O(1)–Zn(1)–O(3W)	88.5 (3)	N(2)–Zn(3)–O(3)	79.7 (3)
N(3)–Zn(1)–O(3W)	89.9 (3)	N(4)#4–Zn(3)–O(3)	102.2 (2)
O(4)–Zn(1)–O(3W)	176.6 (2)	O(8)#4–Zn(3)–O(3)	173.3 (2)
O(4W)–Zn(1)–O(3W)	88.1 (3)		

Note: Symmetry codes for **1**: #1 $y+1/2$, $-x+3/2$, $z+1/4$; #2 y, x, $-z+2$; #3 $-y+3/2$, $x-1/2$, $z-1/4$; for **2**: #1 $x-1/2$, $-y+1/2$, $-z$; #2 $-x+1/2$, $-y+1$, $z-1/2$; #3 $-x+1/2$, $-y+1$, $z+1/2$; #4 $x+1/2$, $-y+1/2$, $-z$.

$EIDC^{3-}$ anions. The axial Co–O bond distances (2.004(5) and 2.073(4) Å) are slightly shorter than the equatorial Co–O/N bond distances, which range from 2.088(6) to 2.142(5) Å. Around Co1, the three *trans* angles are not less than 162° and the *cis* angles range from 78.9(2)° to 108.3(3)°, indicating distortion of the Co1 octahedral environment. Co1 is chelated by two $EIDC^{3-}$ anions and is also coordinated with two waters in a *cis*-configuration; this results in metal-centered chirality, i.e. Co1 has a left-handed screw (Λ) configuration [53]. Co2 adopts a distorted trigonal bipyramidal coordination geometry and is coordinated in the equatorial plane by one water (O3w) and N2 and N2b (symmetry code: b, y, x, $2-z$) from two symmetrical equivalent $EIDC^{3-}$ anions. The axial positions

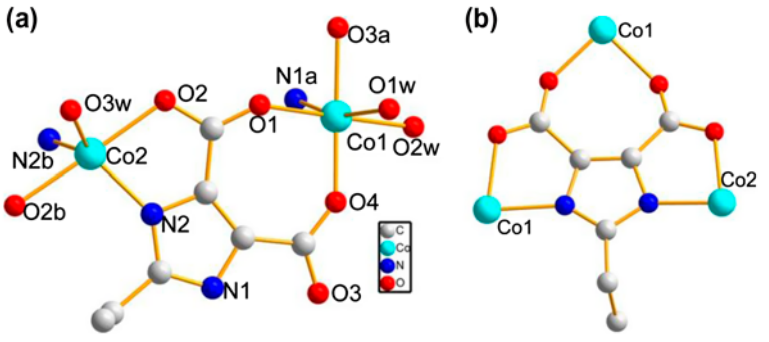

Figure 1. (a) Coordination environment of Co^{II}. (b) Coordination mode of $EIDC^{3-}$ in **1**. Hydrogens are omitted for clarity.

are occupied by carboxylate O2 and O2b. The axial Co–O bond distance (2.148(5) Å) is longer than the equatorial Co–Ow (1.984(7) Å) and Co–N (2.002(6) Å) bond distances. The only *trans* angle is 177.7(3)° and the *cis* angles range from 79.6(2)° to 121.25(18)°, indicating distortion of the Co2 trigonal bipyramidal environment. All these Co−N and Co−O bond lengths are comparable to those in reported imidazole-based dicarboxylate Co(II) complexes $[Co(H_2pimdc)_2(H_2O)_2]\cdot 2DMF$, $[Co(H_2pimdc)_2(H_2O)_2]\cdot 4H_2O$ (H_3pimdc = 2-propyl-4,5-imidazoledicarboxylic acid), and $Co_3(tmidc)_2(H_2O)_4]\cdot(H_2O)_4$ (**3**) [37, 40]. Each $EIDC^{3-}$ connects two Co1 and one Co2 ions in μ_3-(κ^6 *N*1, *N*2, *O*1 : *O*2 : *O*3 : *O*4) coordination [figure 1(b)].

Co1 ions are connected by $EIDC^{3-}$ anions to form a left-handed helical chain along a crystallographic 4_3 screw axis in the [001] direction, with a pitch of 21.870(4) Å [figure 2(b)]. The helical chains are connected by Co2 bridges to form a 3-D homochiral network; each helical chain is surrounded by four symmetrically equivalent helical chains via Co2 centers [figure 2(a)]. In the 3-D network, adjacent four helical chains form a rectangular channel with dimensions of 4.36 × 15.93 Å, in which the coordinated waters are located along the *c* axis. Adjacent rectangular channels are perpendicular to one another. O3w and two Co $(H_2O)_2$ units constructed by Co1, O1w, and O2w are connected into a seven-membered ring, then these rings are interconnected into a 1-D metal–water chain. Each metal–water chain joins four adjacent ones into a 3-D metal–water network (figure 3) [54], further stabilizing the 3-D framework of **1**. The framework of **1** contains two crystallographically independent Co^{2+} ions; however, both of them only coordinate to two $EIDC^{3-}$ ligands, so the Co^{2+} ions can be regarded from the perspective of network topology simply as linkers. Each $EIDC^{3-}$ interacts with three Co^{2+} cations and can be regarded as a 3-connected node. Thus, the framework of **1** may be simplified into a 3-D 3-connected net with $SrSi_2$ topology (figure 4), as determined by *TOPOS* [55].

Comparison of **1** with the recently reported homochiral **3**, which also crystallizes in the tetragonal chiral space group $P4_32_12$ [40], shows that both five- and six-coordinate Co centers are involved in coordination with organic linkers in **1**, while only six-coordinate Co centers exist in **3**. The formation of channels in **3** is dependent on intertwining helical chains; however, the chiral chains in **1** can be viewed as pillars that are connected to each other by Co2 bridges and form 1-D channels. The topology net for **1** is a uninodal 3-connected net, while that for **3** is a binodal (3,4)-connected net.

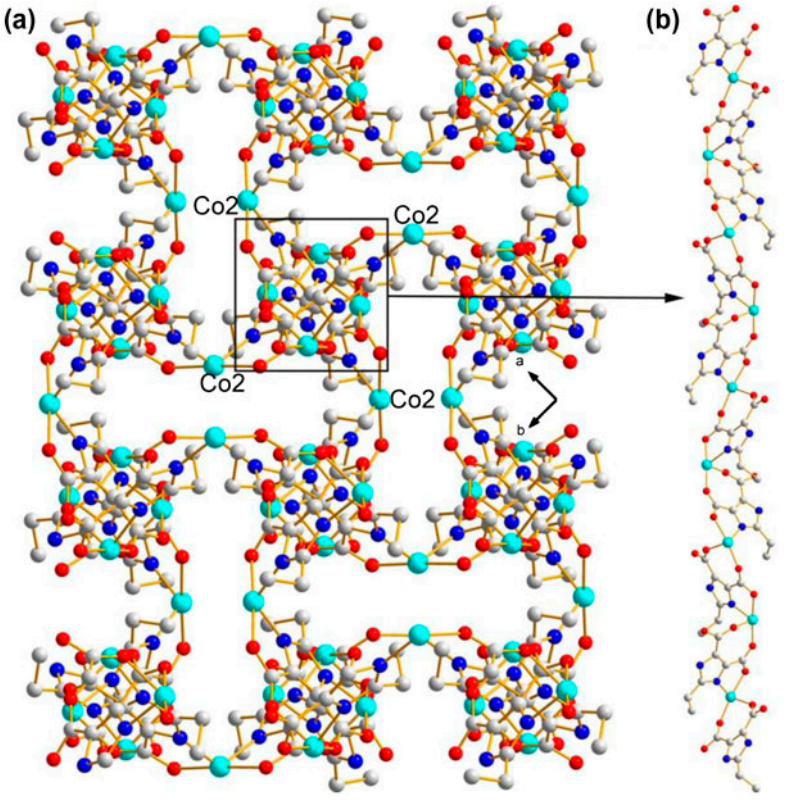

Figure 2. (a) The 3-D homochiral network of **1**; water molecules are omitted for clarity. (b) The helical chain with left-handness.

3.2.2. Crystal structure of 2. X-ray crystallographic data revealed that **2** is also a 3-D homochiral framework and crystallized in the chiral space group $P2_12_12_1$. The asymmetric unit of **2** contains three Zn^{2+} cations, two μ_3-$EIDC^{3-}$, and four coordinated waters. As shown in figure 5(a), Zn1 shows a disordered octahedral coordination geometry where the equatorial plane is occupied by three carboxylate oxygens (O1, O4, and O5) from two different $EIDC^{3-}$ anions and one water (O3w), and the axial sites are occupied by N3 from an $EIDC^{3-}$ and one water (O4w). The Zn–O/N bond distances around Zn1 range from 2.021(5) to 2.170(5) Å, the three *trans* angles are not less than 164°, and the *cis* angles range from 79.1(2)° to 107.5(3)°, indicating distortion of the Zn1 octahedral environment. As opposed to Co1 coordination in **1**, however, Zn1 adopts a right-handed screw (Δ) configuration. Zn2 has a distorted trigonal bipyramidal coordination geometry and is coordinated by N1, carboxylate O7b (symmetry code: b, $0.5-x$, $1-y$, $0.5+z$), and one coordinated water (O2w) in the equatorial plane, while the axial positions are occupied by carboxylate O2 and O6b. The axial Zn–O bond distances (2.020(5) Å for O6b and 2.187(6) Å for O2) are longer than the equatorial Zn–O/N bond distances, which range from 1.984 (7) to 2.002(6) Å. The O6b–Zn–O2 *trans* angle is 171.6(3)° and the *cis* angles subtended at Zn2 are 79.7(2)°–123.3(3)°, indicating distortion of the Zn2 trigonal bipyramidal environment. Similar to Zn2 coordination, Zn3 is also five-coordinate by N2 and N4a (symmetry code: a, $0.5+x$, $0.5-y$, $-z$) from two different $EIDC^{3-}$ anions and one coordinated water

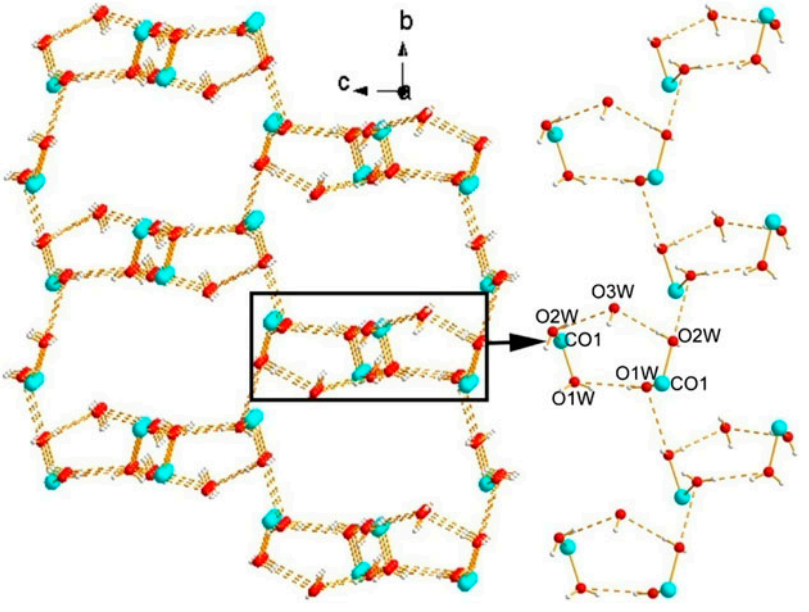

Figure 3. The 3-D metal–water network in **1**.

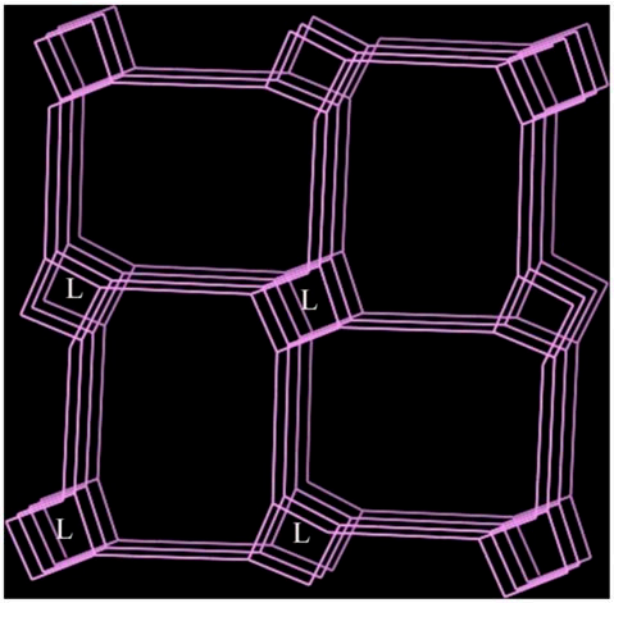

Figure 4. The 3-D 3-connected net with $SrSi_2$ topology.

(O1w) in the equatorial plane, and two carboxylate oxygens (O3 and O8a) in the axial positions, forming a slightly distorted trigonal bipyramidal geometry. The axial Zn–O bond distances (2.149(6) and 2.124(6) Å for O3 and O8a, respectively) are longer than the

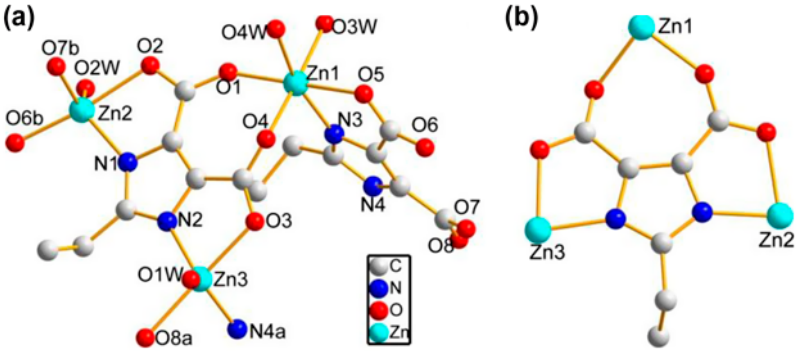

Figure 5. (a) Coordination environment of Zn^{II}. (b) Coordination mode of $EIDC^{3-}$ in **2**. Hydrogens are omitted for clarity.

equatorial Zn–O/N bond distances, which range from 1.985(6) to 2.023(7) Å. The *trans* angle (173.3(2)°) and the *cis* angles ranging from 80.5(2)° to 128.0(3)° indicate distortion of Zn3 trigonal bipyramid. These Zn−N and Zn−O bond lengths are comparable to the reported imidazole-based dicarboxylate Zn(II) complexes $[Zn(EIDC)(phen)]_n$, $[Zn(H_2MIDC)_2(H_2O)_2]$, and $[Zn_3(MIDC)_2(H_2O)_2(DMF)_2]\cdot 0.5H_2O$ [29, 33]. Similar to **1**, each $EIDC^{3-}$ in **2** connects three Zn^{2+} ions in a μ_3-(κ^6 *N*1, *N*2, *O*1 : *O*2 : *O*3 : *O*4) coordination mode [figure 5(b)]. Each $EIDC^{3-}$ coordinates to one five-coordinate and two six-coordinate Zn(II) cations in **1**; however, one six-coordinate and two five-coordinate Zn(II) cations are involved in coordination with one $EIDC^{3-}$ in **2**.

Zn1 and Zn2 are connected by $EIDC^{3-}$ anions to form a right-handed helical chain along the crystallographic 2_1 screw axis in the [0 0 1] direction with a pitch of 22.190(1) Å.

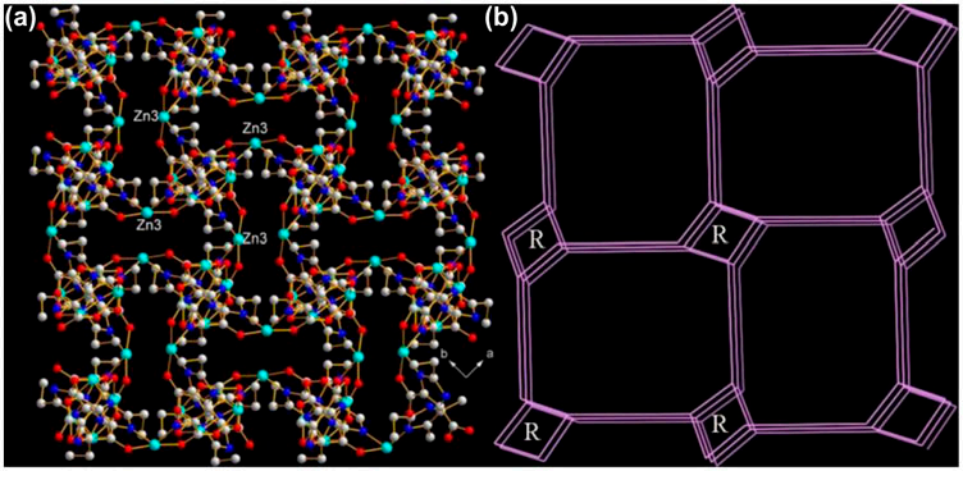

Figure 6. (a) The 3-D homochiral network with right-handness chains; water molecules are omitted for clarity. (b) The 3-D 3-connected net with $SrSi_2$ topology of **2**.

These helical chains are connected to each other by Zn3 bridges to form a 3-D homochiral network with rectangular channels (4.36×15.93 Å^2) along the c axis [figure 6(a)]. While similar homochiral metal–organic frameworks were found in **1** and **2**, they are composed of chiral chains with opposite handedness. Moreover, only a 1-D metal–water chain is formed in **2** (figure S3) rather than 3-D metal–water network of **1**. From the perspective of network topology, the three crystallographically independent Zn^{2+} ions, which only coordinate to two $EIDC^{3-}$ ligands, act simply as linkers. The two kinds of $EIDC^{3-}$ anions interact with three Zn^{2+} ions and can be regarded as 3-connected nodes. So, the framework of **2** may be simplified into a 3-D 3-connected net with $SrSi_2$ topology [figure 6(b)].

The differences between **2** and **3** are similar to those between **1** and **3.** Only six-coordinate Co centers exist in **3;** however, both five- and six-coordinate Zn centers are involved in coordination with the organic linkers in **2**. The right-handed chiral chains are pillars and are connected to each other by Zn3 bridges into 1-D channels in **2**, while the formation of channels in **3** is dependent on intertwining left-handed helical chains. The same differences in network topology between **1** and **2** also hold for **2** and **3**.

3.3. *PXRD of 1 and 2*

The experimental and simulated PXRD patterns of **1** and **2** are shown in figure 7. The simulated PXRD patterns from the single-crystal X-ray diffraction data are in agreement with the observed ones, indicating the phase purity of these synthesized crystalline products. The differences in intensity may be due to the preferred orientation of the powder samples.

3.4. *CD spectra of 1 and 2*

The combination of single-crystal X-ray structure determinations and CD spectra is the most common way of collecting evidence for the homochirality or enantioenrichment of a bulk material. As shown in figure 8, the CD spectrum of **1** exhibits a positive Cotton effect around 216 nm, and a negative Cotton effect with peaks at 280 and 328 nm [48, 49]. The CD spectrum of **2** shows a positive Cotton effect with peaks at 250 and 302 nm, and a negative Cotton effect around 220 nm. These data confirmed that **1** and **2** are chiral compounds, consistent with the crystal structure of the two complexes.

3.5. *TG curves of 1 and 2*

The thermal behavior of **1** and **2** were studied in air from 13 to 700 °C. The TGA analyses (figure 9) revealed that **1** and **2** decompose through two major processes. The first weight loss for **1** and **2** corresponded to that of coordinated water from 26 to 180 °C (Obsd 13.35% for **1**, 10.45% for **2**; Calcd 14.31% for **1**, 11.42% for **2**). The second weight loss for **1** and **2** is a characteristic of combustion of $EIDC^{3-}$. The total weight loss for this step for **1** and **2** amounted to 57.47% and 62.39%, respectively (Calcd 60.42% for **1**, 61.45% for **2**). The remaining weights for **1** and **2** correspond to the formation of Co_2O_3 and ZnO, respectively (Obsd 42.53% for **1**, 37.61% for **2**; Calcd 39.58% for **1**, 38.55% for **2**).

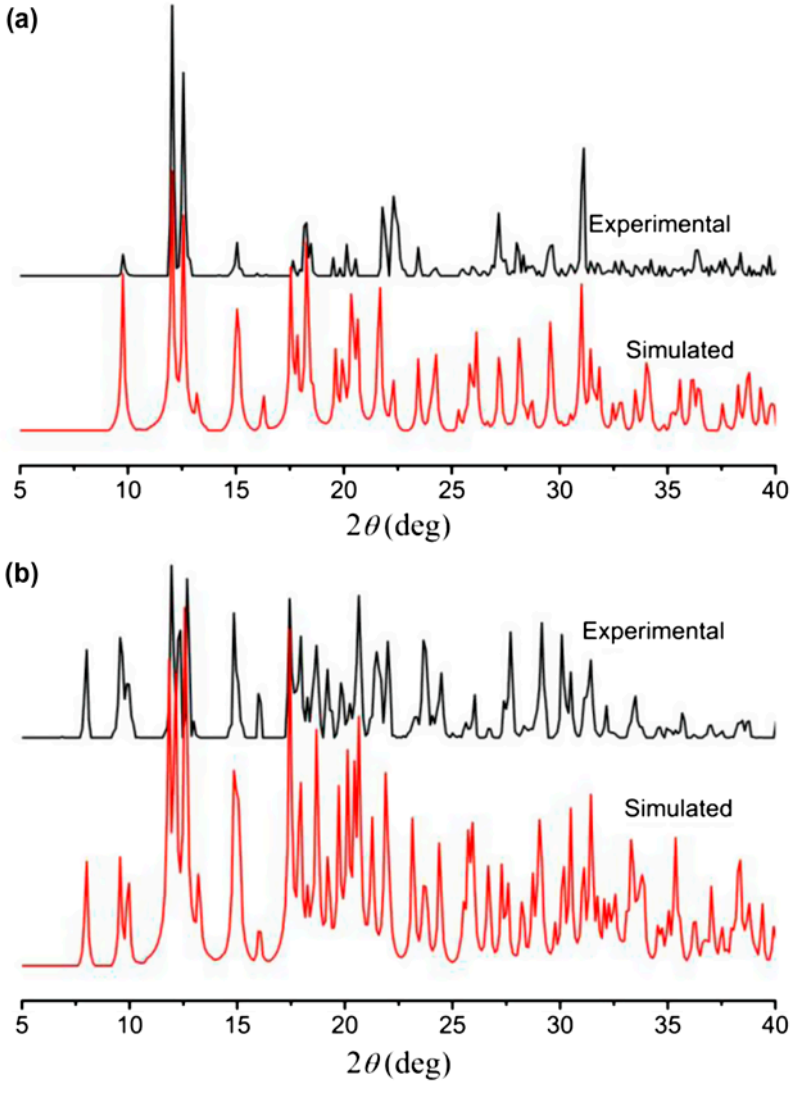

Figure 7. Experimental and simulated X-ray diffraction patterns of **1** (a) and **2** (b).

3.6. *Magnetic properties of 1*

The temperature dependence of the magnetic susceptibility of **1** is shown in figure 10. Upon lowering the temperature, $\chi_m T$ values decreased gradually from 5.82 $cm^3\,K\,M^{-1}$ at 300 K to a minimum of 2.85 $cm^3\,K\,M^{-1}$ at 7 K and then increased to 3.0 $cm^3\,K\,M^{-1}$ at 5.5 K. Upon further cooling, the $\chi_m T$ values dropped sharply to 1.61 $cm^3\,K\,M^{-1}$ at 2 K. The increase of $\chi_m T$ between 5 and 7 K is probably due to spin-canting behavior [56, 57]. The χ_m^{-1} *versus* T curve shows Curie–Weiss law behavior between 30 and 300 K, with Curie constant $C = 4.71\ cm^3\,K\,M^{-1}$ and Weiss constant $\theta = -34.03$ K. The large negative value of θ and the decrease of $\chi_m T$ with temperature indicate strong antiferromagnetic interactions between Co(II) centers [58, 59].

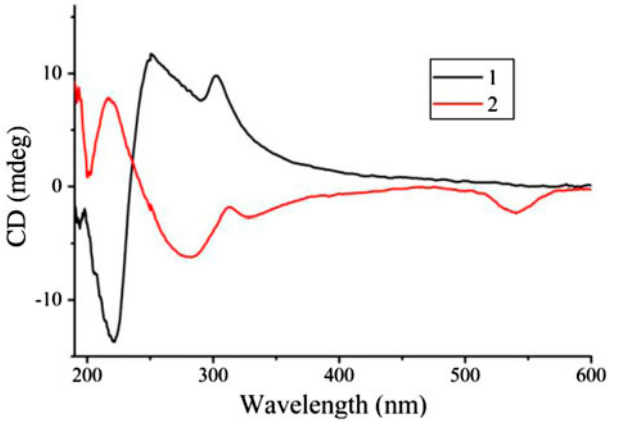

Figure 8. CD spectra of **1** and **2** in the solid state.

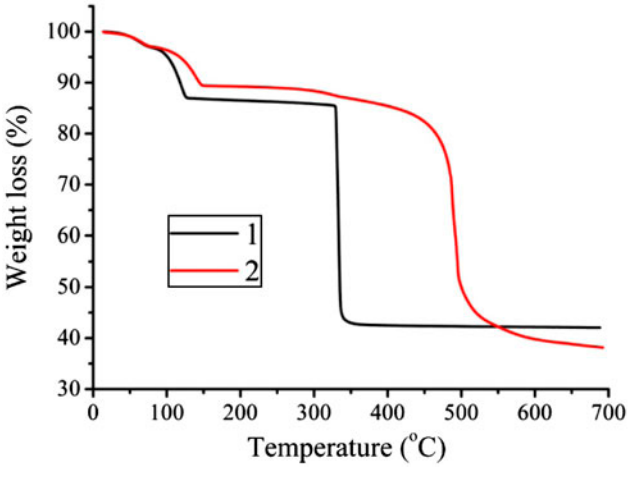

Figure 9. The TG curves of **1** and **2**.

3.7. *PL spectrum of 2*

The PL spectra of H_3EIDC and **2** in the solid state at room temperature are shown in figure 11. The PL spectrum of H_3EIDC revealed an intense fluorescent emission at 425 nm ($\lambda_{ex} = 254$ nm). Similarly, **2** also exhibited blue PL with an emission maximum at 425 upon excitation at 360 nm. Compared with the PL spectrum of H_3EIDC, the emission bands for **2** are very similar to those found for free H_3EIDC in terms of position and band shape. Therefore, the emission bands of **2** are mainly due to an intraligand emission state similar to those reported for d^{10} metal complexes with N-donor carboxylates [60, 61]. Therefore, the emissions of **2** may be assigned to a $\pi^* \rightarrow \pi$ or $\pi^* \rightarrow n$ transition of $EIDC^{3-}$.

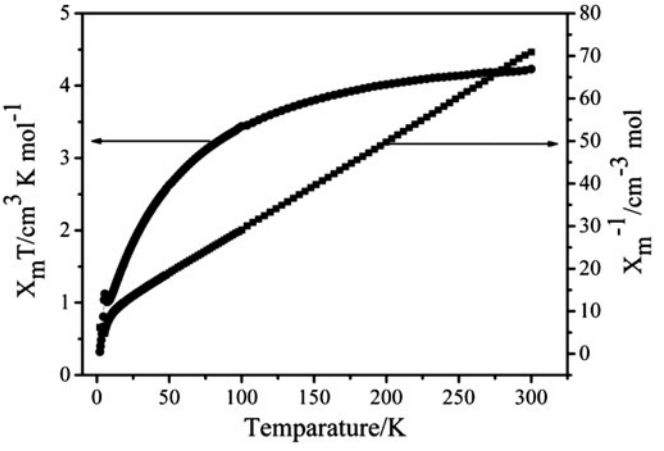

Figure 10. Plots of $\chi_m T$ and χ_m^{-1} *vs.* T for **1**.

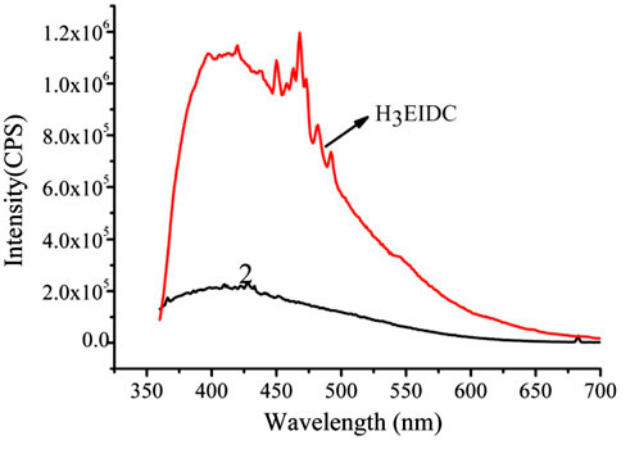

Figure 11. Solid-state emission spectra for **2** and H_3EIDC at room temperature.

4. Conclusion

Two new homochiral complexes, $\{Co_3(EIDC)_2(H_2O)_5\}_n$ (**1**) and $\{Zn_3(EIDC)_2(H_2O)_4\}_n$ (**2**), have been synthesized by spontaneous resolution under solvothermal conditions and fully characterized by elemental analyses, IR, CD, PL spectroscopy, single-crystal X-ray diffraction, TGA, and magnetic analysis. X-ray diffraction revealed that **1** is constructed by left-handed chiral chains; however, right-handed chiral chains constitute the homochiral framework of **2**. The results reveal that formation of a metal ion with left-handed or right-handed configuration, depending on the spatial disposition of the ligands, can result in the formation of homochiral metal–organic frameworks. Further research for the construction of new architectures with more transition metals is underway in our laboratory.

Supplementary material

The geometric parameters of the hydrogen bonds for **1** and **2** (table S1); SEM image and EDS spectrum of the precipitate found in the syntheses of **1** and **2** (figure S1); PXRD pattern of the red crystals found in the synthesis of **1** without DPT (figure S2); and the 1-D metal–water chain of **2** (figure S3). CCDC 916601 and 916602 for **1** and **2** contain the supplementary crystallographic data. These data can be obtained free of charge from The Cambridge Crystallographic Data Center via http://www.ccdc.cam.ac.uk/data_request/cif.

Funding

This work was supported by the National Natural Science Foundation of China [grant number 21201155]; the Natural Science Young Scholars Foundation of Shanxi Province [grant numbers 2012021007-5, 2013021008-6]; Program for the Top Young Academic Leaders of Higher Learning Institutions of Shanxi, respectively.

References

[1] M. Eddaoudi, D.B. Moler, H.L. Li, B.L. Chen, T.M. Reineke, M. O'Keeffe, O.M. Yaghi. *Acc. Chem. Res.*, **34**, 319 (2001).
[2] B.J. Holliday, C.A. Mirkin. *Angew. Chem., Int. Ed.*, **40**, 2022 (2001).
[3] B. Moulton, M.J. Zaworotko. *Chem. Rev.*, **101**, 1629 (2001).
[4] O.M. Yaghi, M. O'Keeffe, N.W. Ockwig, H.K. Chae, M. Eddaoudi, J. Kim. *Nature*, **423**, 705 (2003).
[5] S. Kitagawa, R. Kitaura, S. Noro. *Angew. Chem., Int. Ed.*, **43**, 2334 (2004).
[6] G. Férey. *Chem. Soc. Rev.*, **37**, 191 (2008).
[7] J.R. Li, R.J. Kuppler, H.C. Zhou. *Chem. Soc. Rev.*, **38**, 1477 (2009).
[8] L.Q. Ma, C. Abney, W.B. Lin. *Chem. Soc. Rev.*, **38**, 1248 (2009).
[9] D.J. Tranchemontagne, J.L. Mendoza-Cortés, M. O'Keeffe, O.M. Yaghi. *Chem. Soc. Rev.*, **38**, 1257 (2009).
[10] R. Chakrabarty, P.S. Mukherjee, P.J. Stang. *Chem. Rev.*, **111**, 6810 (2011).
[11] A. Corma, H. García, F.X. Llabrès i Xamena. *Chem. Rev.*, **111**, 4607 (2011).
[12] J.P. Zhang, Y.B. Zhang, J.B. Lin, X.M. Chen. *Chem. Rev.*, **112**, 1001 (2012).
[13] J.R. Li, J.L. Sculley, H.C. Zhou. *Chem. Rev.*, **112**, 869 (2012).
[14] R.Q. Zou, H. Sakurai, Q. Xu. *Angew. Chem., Int. Ed.*, **45**, 2542 (2006).
[15] Y. Liu, V. Kravtsov, R.D. Walsh, P. Poddar, H. Srikanth, M. Eddaoudi. *Chem. Commun.*, 2806 (2004).
[16] C.F. Wang, E.Q. Gao, Z. He, C.H. Yan. *Chem. Commun.*, 720 (2004).
[17] S. Wang, L. Zhang, G. Li, Q. Huo, Y. Liu. *CrystEngComm*, **10**, 1662 (2008).
[18] X.F. Zhang, Z.P. Deng, L.H. Huo, Q.M. Feng, S. Gao. *Eur. J. Inorg. Chem.*, 5506 (2012).
[19] F. Zhang, Z. Li, T. Ge, H. Yao, G. Li, H. Lu, Y. Zhu. *Inorg. Chem.*, **49**, 3776 (2010).
[20] Z.G. Gu, G.Z. Li, P.Y. Yin, Y.N. Chen, H.M. Peng, M.F. Wang, F. Cheng, F.L. Gu, W.S. Li, Y.P. Cai. *Inorg. Chem. Commun.*, **14**, 1479 (2011).
[21] C.X. Meng, D.S. Li, J. Zhao, F. Fu, X.N. Zhang, L. Tang, Y.Y. Wang. *Inorg. Chem. Commun.*, **12**, 793 (2009).
[22] Z. Li, C. Chen, L. Yan, G. Li, C. Wu, H. Lu. *Inorg. Chim. Acta*, **377**, 42 (2011).
[23] Z.F. Li, X.B. Luo, Y.C. Gao, H.J. Lu, G. Li. *Inorg. Chim. Acta*, **384**, 352 (2012).
[24] M.H. Alkordi, Y. Liu, R.W. Larsen, J.F. Eubank, M. Eddaoudi. *J. Am. Chem. Soc.*, **130**, 12639 (2008).
[25] M.H. Alkordi, J.A. Brant, L. Wojtas, V.C. Kravtsov, A.J. Cairns, M. Eddaoudi. *J. Am. Chem. Soc.*, **131**, 17753 (2009).
[26] S. Wang, T.T. Zhao, G.H. Li, L. Wojtas, Q.S. Huo, M. Eddaoudi, Y.L. Liu. *J. Am. Chem. Soc.*, **132**, 18038 (2012).
[27] N. Chen, J. Zhang, Y.C. Gao, Z.L. Yang, H.J. Lu, G. Li. *J. Coord. Chem.*, **64**, 2554 (2011).
[28] M.W. Guo, N. Chen, Y.C. Gao, H.J. Lu, G. Li. *J. Coord. Chem.*, **65**, 1724 (2012).
[29] W.D. Song, S.J. Li, S.W. Tong, D.L. Miao, L.L. Ji, J.B. An. *J. Coord. Chem.*, **65**, 3653 (2012).
[30] Y.G. Sun, M.Y. Guo, G. Xiong, F. Ding, L. Wang, B. Jiang, M.C. Zhu, E.J. Gao, F. Verpoort. *J. Coord. Chem.*, **63**, 4188 (2010).
[31] R.Q. Fan, L.Y. Wang, H. Chen, G.P. Zhou, Y.L. Yang, W. Hasi, W.W. Cao. *Polyhedron*, **33**, 90 (2012).
[32] Y.C. Gao, Q.H. Liu, F.W. Zhang, G. Li, W.Y. Wang, H.J. Lu. *Polyhedron*, **30**, 1 (2011).
[33] J.F. Song, R.S. Zhou, T.P. Hu, Z. Chen, B.B. Wang. *J. Coord. Chem.*, **63**, 4201 (2010).

[34] X. Feng, S.H. Li, L.Y. Wang, J.S. Zhao, Z.Q. Shi, P.P. Lei. *CrystEngComm*, **14**, 3684 (2012).
[35] S.M. Fang, D.L. Peng, M. Chen, L.R. Jia, M. Hu. *J. Coord. Chem.*, **65**, 668 (2012).
[36] T. Li, Y. Xiu, X. Su, X.R. Meng. *J. Coord. Chem.*, **65**, 3111 (2012).
[37] Z.R. Luo, J.C. Zhuang, Q.L. Wu, X. Yin, S.W. Tan, J.Z. Liu. *J. Coord. Chem.*, **64**, 1054 (2011).
[38] D.P. Wang, Y.G. Chen, H.Y. Wang, C.J. Zhang, Q. Tang. *J. Coord. Chem.*, **64**, 2824 (2011).
[39] G. Han, Y. Mu, D.Q. Wu, Y.Y. Jia, H.W. Hou, Y.T. Fan. *J. Coord. Chem.*, **65**, 3570 (2012).
[40] L.X. Xie, X.W. Hou, Y.T. Fan, H.W. Hou. *Cryst. Growth Des.*, **12**, 1282 (2012).
[41] S.L. Xiao, Y.Q. Zhao, C.H. He, G.H. Cui. *J. Coord. Chem.*, **66**, 89 (2013).
[42] L. Zhang, D. Xu, Y. Zhou, Y. Guo, W. Ahmad. *J. Coord. Chem.*, **65**, 3028 (2012).
[43] W.G. Lu, J.Z. Gu, L. Jiang, M.Y. Tan, T.B. Lu. *Cryst. Growth Des.*, **8**, 192 (2008).
[44] Y.Q. Sun, J. Zhang, G.Y. Yang. *Chem. Commun.*, 4700 (2006).
[45] Z.F. Li, L. Guo, F.W. Zhang, G. Li, L. Zhu. *Synth. React. Inorg. Met-Org. Chem.*, **40**, 734 (2010).
[46] R. Banerjee, A. Phan, B. Wang, C. Knobler, H. Furukawa, M. O'Keeffe, O.M. Yaghi. *Science*, **319**, 939 (2008).
[47] B. Wang, A.P. Côté, H. Furukawa, M. O'Keeffe, O.M. Yaghi. *Nature*, **453**, 207 (2008).
[48] K.K. Bisht, E. Suresh. *J. Am. Chem. Soc.*, **135**, 15690 (2013).
[49] Z. Su, M.S. Chen, J. Fan, M. Chen, S.S. Chen, L. Luo, W.Y. Sun. *CrystEngComm*, **12**, 2040 (2010).
[50] G. Tsukamoto, K. Yoshino, T. Kohno, H. Ohtaka, H. Kagaya, K. Ito. *J. Med. Chem.*, **23**, 738 (1980).
[51] G.M. Sheldrick. *SHELXS 97, Program for Crystal Structure Refinement*, University of Göttingen, Germany (1998).
[52] A.L. Spek. *PLATON, Molecular Geometry Program*, University of Utrecht, The Netherlands (1999).
[53] J.J. Jodry, R. Frantz, J. Lacour. *Inorg. Chem.*, **43**, 3329 (2004).
[54] B.H. Ye, B.B. Ding, Y.Q. Weng, X.M. Chen. *Inorg. Chem.*, **43**, 6866 (2004).
[55] V.A. Blatov, A.P. Shevchenko, V.N. Serezhkin. *J. Appl. Cryst.*, **33**, 1193 (2000).
[56] X.Y. Wang, L. Wang, Z.M. Wang, G. Su, S. Gao. *Chem. Mater.*, **17**, 6369 (2005).
[57] H.H. Ko, J.H. Lim, H.C. Kim, C.S. Hong. *Inorg. Chem.*, **45**, 8847 (2006).
[58] Y.F. Bi, X.T. Wang, W.P. Liao, X.F. Wang, X.W. Wang, H.J. Zhang, S. Gao. *J. Am. Chem. Soc.*, **131**, 11650 (2009).
[59] M.H. Zeng, Y.L. Zhou, M.C. Wu, H.L. Sun, M. Du. *Inorg. Chem.*, **49**, 6436 (2010).
[60] S.L. Zheng, J.H. Yang, X.L. Yu, X.M. Chen, W.T. Wong. *Inorg. Chem.*, **43**, 83 (2004).
[61] X. Li, B.L. Wu, C.Y. Niu, Y.Y. Niu, H.Y. Zhang. *Cryst. Growth Des.*, **9**, 3423 (2009).